IOP Publishing Superconductor Science and Technology
Supercond. Sci. Technol. 31 (2018) 055009 (8pp) https://doi.org/10.1088/1361-6668/aab585

Novel model of stator design to reduce the mass of superconducting generators

Kevin Kails, Quan Li and Markus Mueller

School of Engineering, Institute for Energy Systems, The University of Edinburgh, United Kingdom

E-mail: quan.li@ed.ac.uk

Received 29 November 2017, revised 5 March 2018
Accepted for publication 9 March 2018
Published 4 April 2018

Abstract

High temperature superconductors (HTS), with much higher current density than conventional copper wires, make it feasible to develop very powerful and compact power generators. Thus, they are considered as one promising solution for large (10 + MW) direct-drive offshore wind turbines due to their low tower head mass. However, most HTS generator designs are based on a radial topology, which requires an excessive amount of HTS material and suffers from cooling and reliability issues. Axial flux machines on the other hand offer higher torque/volume ratios than the radial machines, which makes them an attractive option where space and transportation becomes an issue. However, their disadvantage is heavy structural mass. In this paper a novel stator design is introduced for HTS axial flux machines which enables a reduction in their structural mass. The stator is for the first time designed with a 45° angle that deviates the air gap closing forces into the vertical direction reducing the axial forces. The reduced axial forces improve the structural stability and consequently simplify their structural design. The novel methodology was then validated through an existing design of the HTS axial flux machine achieving a ~10% mass reduction from 126 tonnes down to 115 tonnes. In addition, the air gap flux density increases due to the new claw pole shapes improving its power density from 53.19 to 61.90 W kg^{-1}. It is expected that the HTS axial flux machines designed with the new methodology offer a competitive advantage over other proposed superconducting generator designs in terms of cost, reliability and power density.

Keywords: superconducting generator, direct drive, wind energy, mass reduction

(Some figures may appear in colour only in the online journal)

1. Introduction

One of the challenges the wind energy sector is facing is to reduce the cost of energy. For several decades there has been a trend towards higher power-rated wind turbines, which help reduce the cost of energy through lowering installation and maintenance costs per kWh [1]. Projections indicate that 85% of offshore wind turbines will be rated above 5 MW in 2020 [2]. However, one critical issue with large wind turbines is the tower head mass. The tower head becomes extremely heavy for large wind turbines, which leads to an urgent need for more robust foundation towers that dramatically increase the cost of the whole system [3]. To solve this issue a novel lighter topology of power generators based on high temperature superconductors (HTS) is required which would enable 10 MW and even higher rated wind turbines. Based on previous research a reduction of weight of at least 30% when compared to conventional power generators is possible [4]. It has also been shown that HTS machines remain extremely efficient even when only operating under partial load [5]. This is an attractive feature for wind turbines since they often operate below rated power due to lower wind speeds. There are several other superconducting power generator designs for wind turbines available and the vast majority are based on the radial rather than axial configuration [6–14]. Most of these machines suffer from reliability issues due to rotating superconducting field windings. In addition, they use an excessive amount of superconducting tape, usually above several hundreds of kilometres, which makes them uneconomical [15]. The closest comparable design to the double claw pole generator is AMSC's 10 MW superconducting generator that uses 36 km of YBCO tape at 30 K [6]. One issue with the double

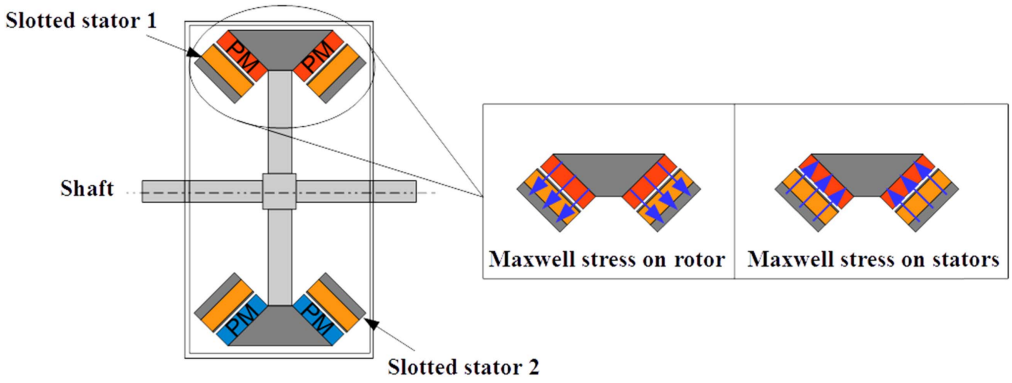

Figure 1. Schematic of a slotted axial flux machine with double stator and internal rotor (left) and Maxwell stress acting on components (right).

Table 1. Comparison of superconducting 10 MW generator designs.

Developer	Topology	Diameter (m)	Weight (tonnes)	SC type	SC length (km)	Temperature (K)
AMSC [6]	Iron-cored SM	4.5–5	180[a]	YBCO	36	30
Sung *et al* [7]	Iron-cored SM	5.3	147[a]	YBCO	586	20
Abrahamsen *et al* [8]	Iron-cored SM	4.7	88	YBCO	200–300	20
Kostopoulos *et al* [9]	Fully SC air-cored SM	5.6	60–70	MgB_2	55	20
Tecnalia [10]	Iron-cored SM	5	161	MgB_2	153	20
Kim *et al* [11]	Air-cored SM	3	41.7	YBCO	289	22
Terao *et al* [12]	Fully SC air-cored SM	3.67	31.7	MgB_2 + HTS	270	20
General Electric [13]	Air-cored SM	4.87	143[a]	NbTi	720	6
Kalsi [14]	Fully SC air-cored SM	5	52.4	MgB_2	42.6	20

[a] With structural mass (SM).

claw pole generator is however that it is still too heavy to satisfy the needs of the future wind industry market. Table 1 lists several 10 MW superconducting generator designs for wind turbines that were published in recent years. It can be seen there is a wide spread in diameter, weight and superconductor requirements from different designs. Since the double claw pole machine is heavy, further investigation into the mass reduction is required.

2. Novel stator design for axial flux machines

In an axial flux machine, the magnetic flux travels axially across the air gap. The main advantage of axial flux machines is that they offer higher torque/volume ratios than other topologies which make them an attractive option where space or transportation becomes an issue [16]. However, since the flux crosses the air gap in the axial direction there are large axial forces acting on the machine components leading to structural instability. To counter this, axial flux machines require a rigid structure, which in turn leads to a lower torque/mass ratio [17]. In addition, due to the large magnetomotive force (MMF) produced by superconductors, machine structure should be precisely designed to ensure the air gap clearance is maintained at all times. The air gap closing force can be expressed as shown in (1)

$$F = \frac{B^2 A}{2\mu_0}, \tag{1}$$

where B is the air gap flux density, A is the cross-sectional area of the air gap and μ_0 is the magnetic permeability of air. Conventional machines tend to only operate with an air gap flux density of 0.6–0.8 T. Superconducting machines on the other hand can easily reach and exceed 1 T leading to very high air gap closing forces.

These issues in conjunction with superconductors make the design of axial flux machines very challenging. Figure 1 shows a schematic of an axial flux machine with double slotted stators and a single rotor. It is one of the most common types of axial flux machines next to variation with double rotors and a single stator [17]. The Maxwell stress on the machine components is highlighted. While the forces on the rotor are balanced, the forces on the stator sides are not and they only act in the axial direction. In conjunction with very large diameter machines, it is challenging to maintain the air gap clearance.

It was already discussed that there are large forces acting on the machine components, these are difficult to handle and increase the structural mass of the machine. A high air gap flux density is however required in order to achieve a high power density. From (2) it can be see that the power output of a machine is proportional to the air gap flux density

$$P = BA_E \frac{\pi}{2} D^2 L \omega, \tag{2}$$

where B is the air gap flux density, A_E is the electric loading, D is the machine air gap diameter, L is axial length of the

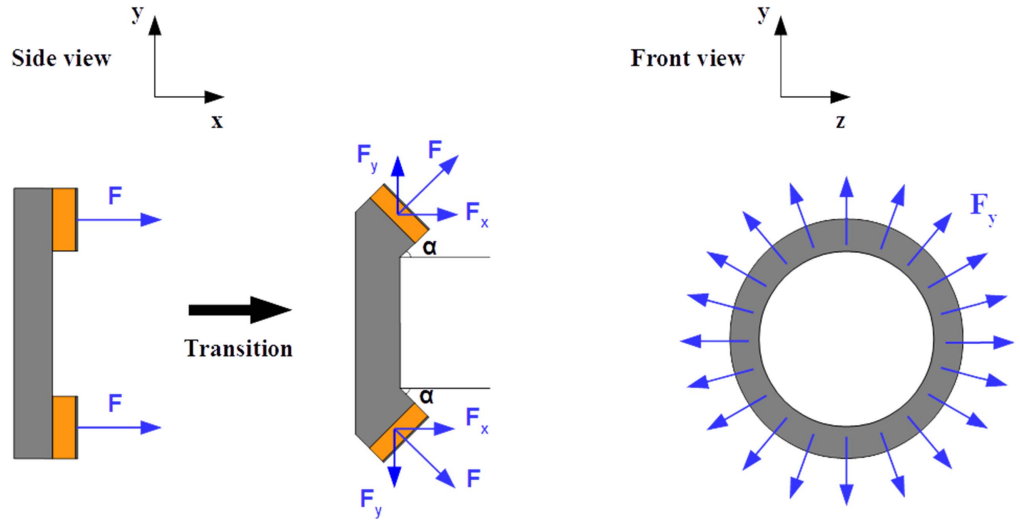

Figure 2. Novel stator design for axial flux machines: side view of the stator (left) and front view of the stator (right).

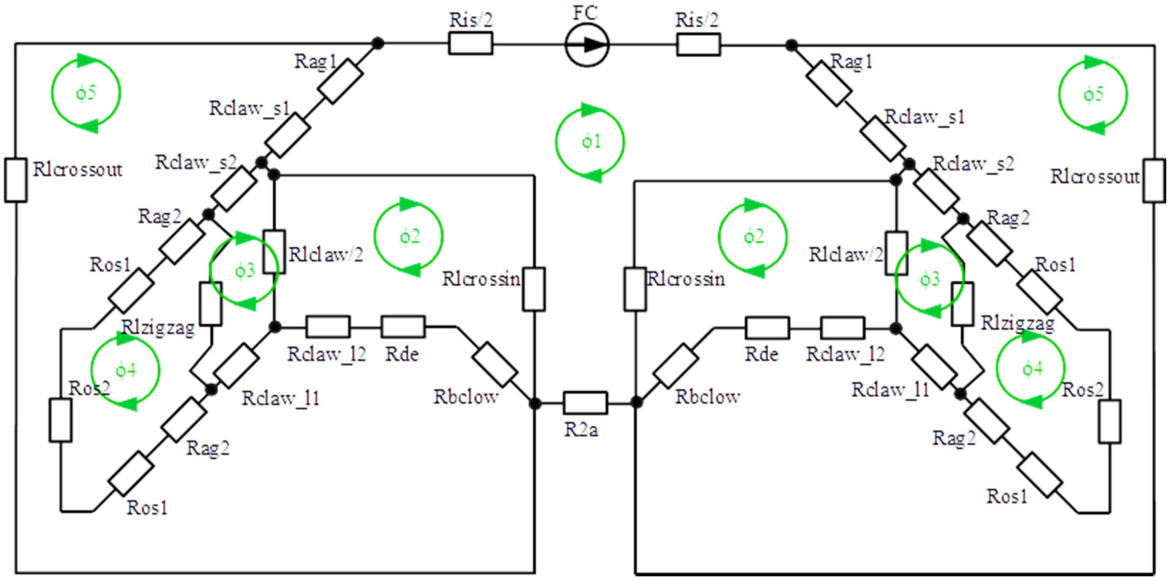

Figure 3. Reluctance network of the double claw pole machine with angled stator sides.

Table 2. Original design of the double claw pole generator.

Attribute	Value
Total mass	188 tonnes
Outer diameter	6.37 m
Power output	10 MW
Rotational speed	10 rpm
Power density	53.19 W kg^{-1}
HTS requirement at 30 K	3.3 km

machine and ω is the rotational speed. Since an iron-cored structure is desired to avoid using an excessive amount of superconducting tape, the air gap closing forces cannot be avoided without decreasing the machine's performance. Clearly, the force itself cannot be reduced, the direction of the force however can be diverted, which is achievable by designing the stator with an angle. Figure 2 shows a schematic of the concept. The stator teeth are angled outwards by an angle α deviating the air gap closing forces. The angle α is used to adjust the axial and radial forces in order to reduce structural mass. The optimal angle depends on the structure of the machine that the concept is being applied to.

With the angled stator the total air gap closing force can be separated into its x- and y-components as shown in the following equations

$$F_x = F\cos(\alpha), \tag{3}$$

$$F_y = F\sin(\alpha). \tag{4}$$

Through applying an angle to the stator, the axial forces can be reduced and hence the structural stability can be

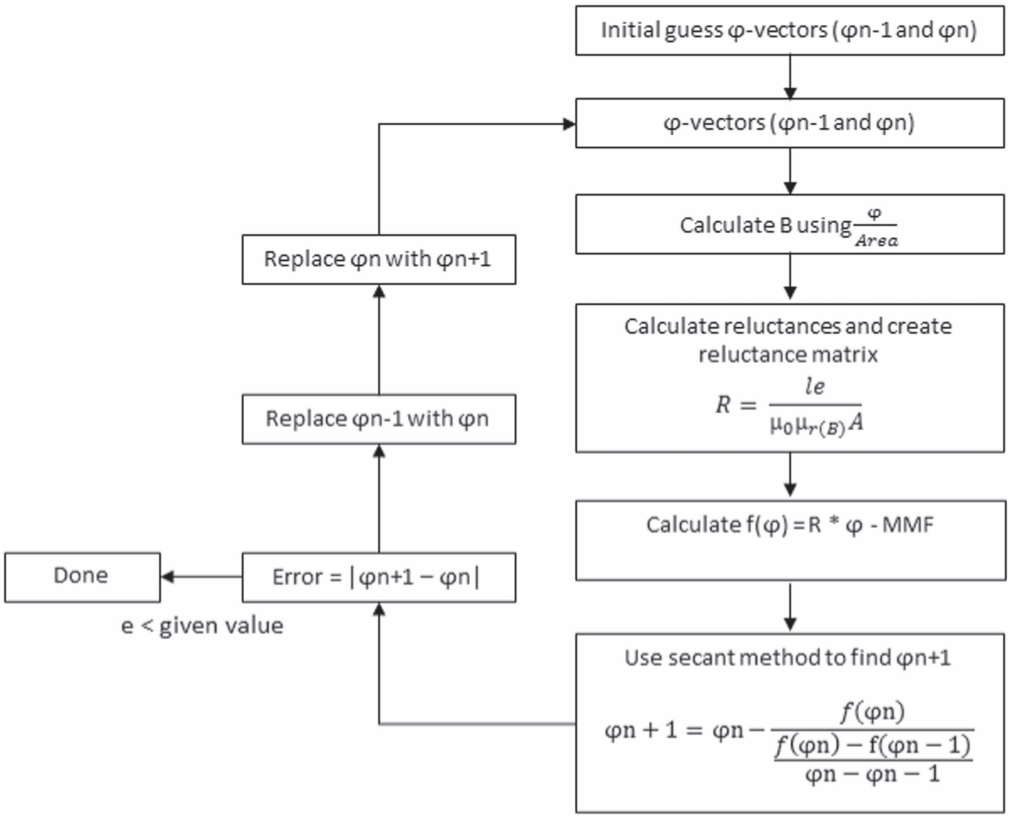

Figure 4. Flow chart of the algorithm used to solve the nonlinear flux loop equations.

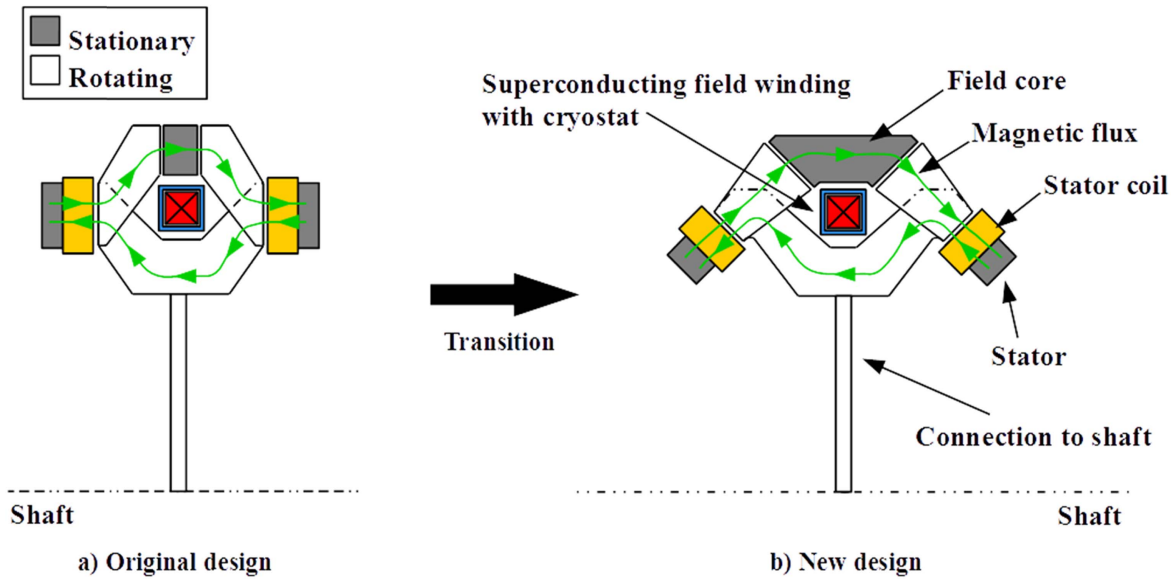

Figure 5. The transition from the (a) original design to (b) the new design.

improved. In order to verify the idea, the concept is applied to the double claw pole machine to reduce its structural mass.

3. Design of the generator

The machine was designed in a manner to keep the critical parameters of the machine approximately the same as for the original design. The main properties are shown in table 2 [4].

Particular attention had to be paid to the dimensions of the claw poles in order to avoid saturation. Another important parameter was to maintain the space in between the claw poles where the superconducting winding and its cryostat are located. In order to model the machine, a reluctance network

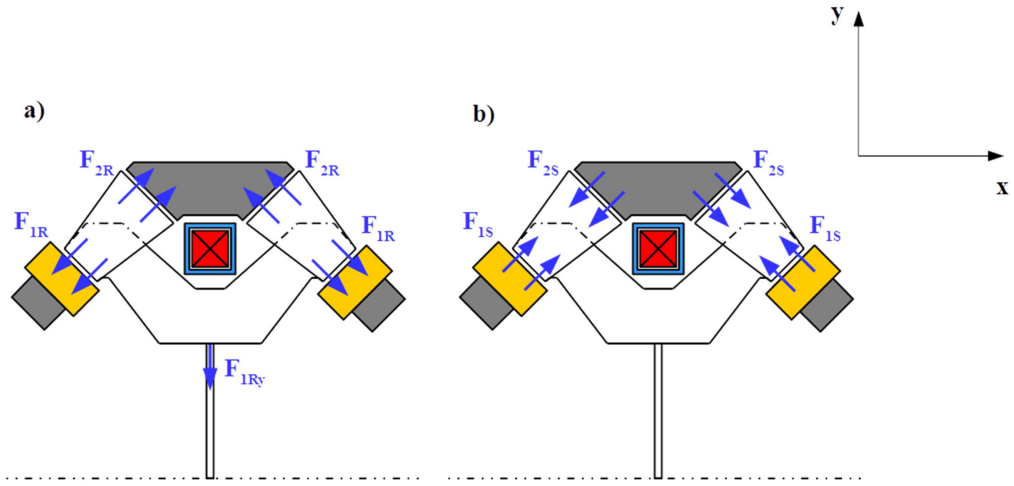

Figure 6. (a) Forces acting on the rotor (claw poles) and (b) forces acting on the stator.

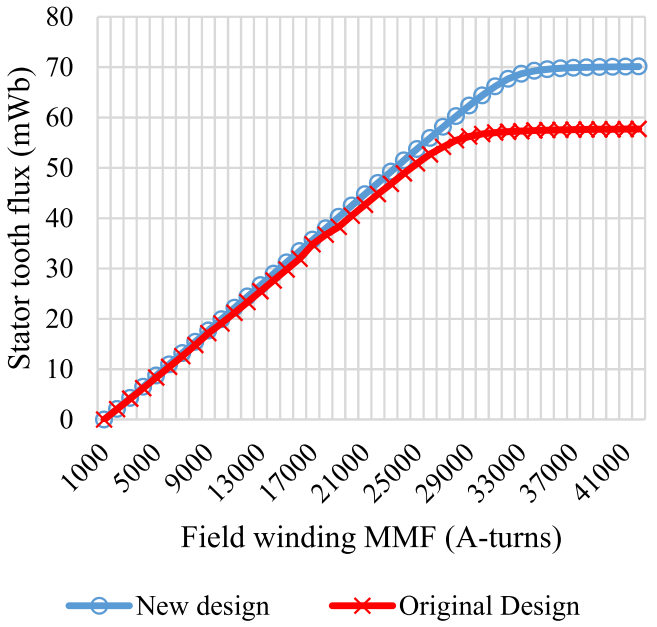

Figure 7. Stator tooth flux variation with MMF for the original and new design.

model based on [18–20] was developed in MATLAB and is shown in figure 3.

From the reluctance network the stator tooth flux can be found. The stator tooth flux is then used to calculate the induced voltage and hence the output power is calculated. Each component of the machine is represented by several reluctances. Each reluctance is calculated according to its geometry and material properties using (5)

$$R = \frac{l_e}{\mu_0 \mu_r A}, \tag{5}$$

where l_e is the equivalent length through the component, μ_0 is the permeability of air, μ_r is the permeability of iron and A is the cross-sectional area of the component. All major leakage flux paths were considered such as, leakage flux between adjacent claw poles, leakage flux from smaller claw poles downwards to the large claw pole and vice versa and zig zag leakage flux between the stator teeth. It was decided to use Vacoflux50 for the active mass due to its high saturation limit of 2.28 T at 16 kAm^{-1} [21]. It is a cobalt iron alloy, which is relatively expensive in comparison to other electrical steels. However, it allows high air gap flux densities without using an excess amount of superconducting tape. In addition, Vacoflux50 can be manufactured in laminations. Hence, even large machine components can be assembled. Since the permeability of iron varies nonlinearly in relation to flux density, an iterative method had to be developed to find the correct flux density for each component. An algorithm based on the Newton–Raphson method, shown in figure 4, was created to solve the nonlinear flux equations.

From the stator tooth flux the induced voltage can be calculated using Faraday's law as shown in (6)

$$E_{\mathrm{RMS}} = \frac{N_{\mathrm{TURN}} \times \phi_{\mathrm{PEAK}} \times f}{\sqrt{2}}, \tag{6}$$

where N_{TURN} is the number of turns per stator coil, Φ_{PEAK} is the peak stator tooth flux and f is the electrical frequency.

I_{RMS} is calculated using (7)

$$I_{\mathrm{RMS}} = J_{\mathrm{RMS}} \times A_{\mathrm{COIL}}, \tag{7}$$

where J_{RMS} is the current density of copper which is assumed to be 5×10^6 A m^{-2} and A_{COIL} is the area of a stator coil.

Using equations (6) and (7) the power output of the generator is calculated as:

$$P_{\mathrm{OUT}} = N_{\mathrm{COIL}} \times (E_{\mathrm{RMS}} \times I_{\mathrm{RMS}} - {I_{\mathrm{RMS}}}^2 \times R_{\mathrm{COIL}}), \tag{8}$$

where N_{COIL} is the number of coils per stator, E_{RMS} is the induced voltage for one coil, I_{RMS} is the stator current and R_{COIL} is the resistance of a stator coil.

The reluctance network model was then used to optimize the new design parameters for the lowest active mass possible. In order to confirm the results from the reluctance network model, a magnetostatic finite element analysis (FEA) was performed using *Infolytica MagNet*.

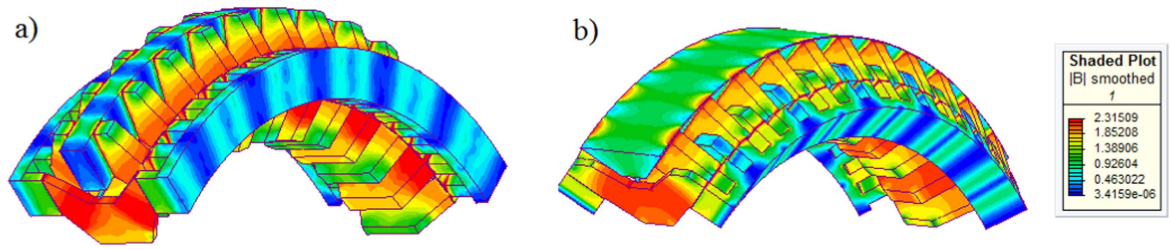

Figure 8. Flux density distribution for (a) the original design and (b) the new design.

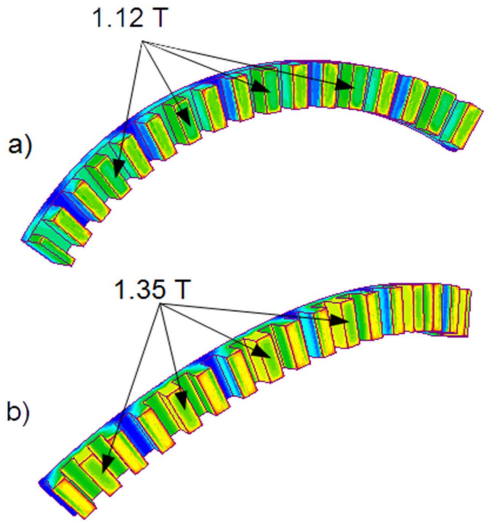

Figure 9. Air gap flux density for (a) the original design and (b) the new design.

4. Results and analyses

The new stator design was applied to the double claw pole machine. Figure 5 shows the transition from the original to the new design. The concept of the double claw pole machine remains the same. The stationary superconducting field winding is supplied with a DC current hence it produces a magnetic field. Upper and lower claw poles are oriented around the field winding. These are oriented in an alternating fashion in order to create a north–south pole flux variation across the stator coils. The stationary field core offers support and access to the superconducting field winding and its cryostat.

From figure 5 it can be seen that for the new design the flux travels axially as well as transversely across the air gaps leading to the forces being diverted. The new directions of the forces acting on the machine components are shown in figure 6.

For the original design [4], the shape of the claw poles was optimized using a genetic algorithm. The cross-sectional areas of the claw poles were increased near the field core to balance the forces F_1 and F_2. These dimensions were taken over for the new design to keep the same balance of forces. In the original design, there was a momentum acting on the small claw poles since the forces did not act on the same plane. For the new design this momentum was eliminated which simplifies the structural design of the rotor. There is a net force inwards from the large claw poles towards the shaft. However, due to the rotational symmetry of the machine these forces are balanced in relation to the shaft leading to no resultant force. This inward force is similar to the forces present in radial flux machines. The x-component of F_1 is smaller in magnitude than the axial force of the original design. Hence the axial forces acting on the stator sides were reduced, improving the structural stability of the machine. Considering the structure of the double claw pole machine, setting the stator sides at an angle of 45° was found to be a good compromise between reducing the axial forces and viability of the design. Increasing the angle further leads to difficulty in maintaining the required space in between the claw poles for the superconducting field winding and its cryostat. In addition, a higher angle would also lead to a stronger bend of the lower claw poles and stator sides, which would increase the manufacturing complexity of the generator components. The reluctance network model highlighted in the previous section was used to optimize the machine. Figure 7 shows the stator tooth flux variation with MMF for the original design and the new optimized design.

It can be seen that the stator tooth flux was increased due to the new shape of the claw poles, which allows them to carry more flux before saturating. The machine was designed for a field winding MMF of 32.4 KA/turn. This is equivalent to 1.45 km (81 turns) of tape at 30 K with a current of 400 A. 5 mm wide YBCO tape is used which has a critical current of 504 A, leaving a safety margin of 25%. The tapes were stacked next to each other, which formed a required conductor area of 15 mm by 32 mm. Similarly, to the original design the field winding can be wound into four separate loops with separate cryostats in order to improve the modularity of the machine [4]. For this configuration the required amount of tape is equivalent to 3.3 km. For a field winding MMF of 32.4 KA/turn the peak stator tooth flux for the original design is equivalent to 57 mWb. For the same MMF the stator tooth flux with the new design was increased to 69 mWb.

In addition to the reluctance network model a magnetostatic analysis using *Infolytica Magnet* was performed. Figure 8 shows the flux density distribution in the machine for the original and new design.

Figure 9 shows the air gap flux density in the middle of the tooth when the large claw pole is aligned. There is a very good agreement between the reluctance network and the FEA results. From the reluctance network model, the air gap flux density was found to be 1.1 T for the original design and

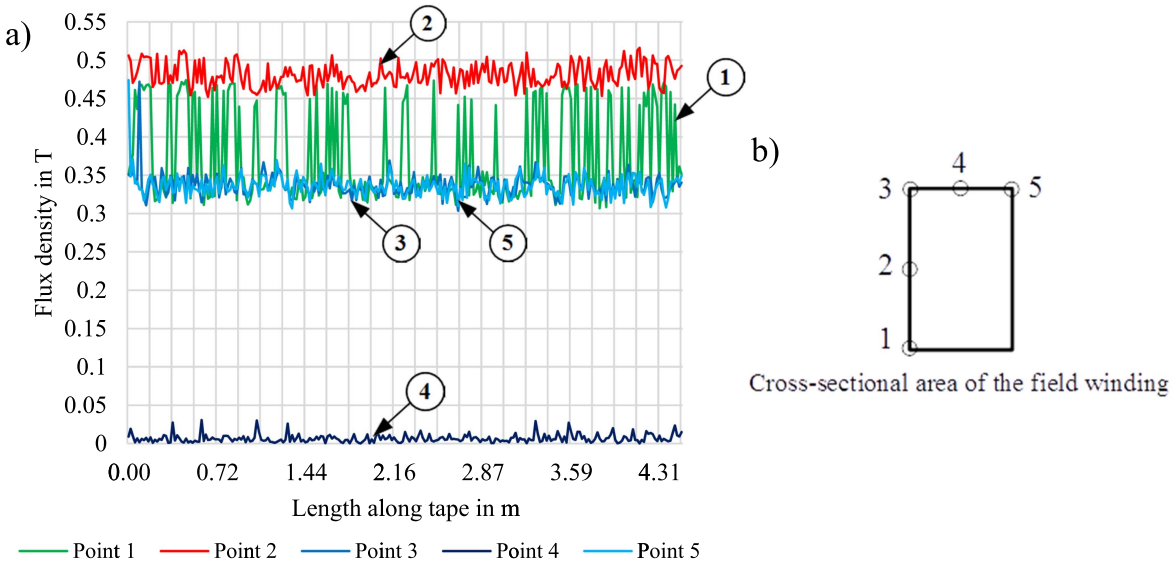

Figure 10. (a) Perpendicular magnetic fields along the superconducting winding and (b) positions of the fields.

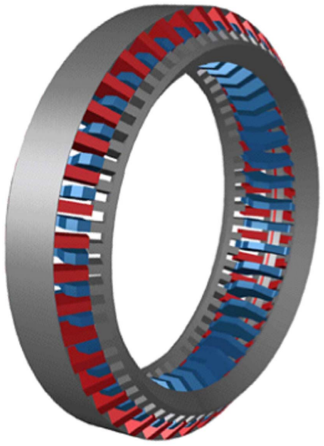

Figure 11. 3D representation of the newly proposed design without the support structure.

Table 3. Design comparison.

Attribute	Components	Original	New
MMF	HTS field winding	Identical	
Mass	Active mass	62 tonnes	74 tonnes
	Structural mass	126 tonnes	115 tonnes
	Total generator	188 tonnes	189 tonnes
Dimensions	Outer diameter	6.37 m	6.14 m
	Axial length	1.34 m	1.72 m
Performance	Power output	10 MW	11.7 MW
	Rotational speed	10 rpm	10 rpm
	Power density	53.19 W kg^{-1}	61.90 W kg^{-1}

1.33 T for the new design. The results from the FEA are 1.12 T and 1.35 T respectively for the original and the new design. The stator tooth flux can be calculated to be 71.4 mWb for a MMF of 32.4 KA/turn similar to the flux shown in figure 7.

Figure 10 shows the perpendicular magnetic field along the superconducting field winding. The magnetic fields at five points along the circumference have been examined. The strongest perpendicular field is found along the edges of the tapes, and the field in the middle of the tape is relatively low. This is very similar to the original design. Hence, the main losses are expected to occur around the edges of the superconducting tapes. Our future work is to quantify the loss in the superconducting winding.

Due to the new design and the increased air gap flux density the structural mass needs to be recalculated. Using an analytical model developed by Zavvos [22] the structural mass can be estimated for the new design. The Maxwell stress is calculated using the air gap flux density highlighted in figure 9(b). The required structure to maintain the air gap clearance is then calculated. It is assumed that there are five torque arms on the rotor and stator [23]. From the analytical model the structural mass was estimated to be 115 tonnes. Figure 11 shows a 3D representation of the design of the double claw pole generator.

Table 3 compares the main aspects of the original and new design. The structural mass was reduced from 126 tonnes down to 115 tonnes due to the deviated air gap closing forces. The power density of the generator was increased from 53.19 to 61.90 W kg^{-1} while maintaining the same HTS tape requirements.

In order to make a meaningful comparison between the two concepts the rotational speed as well as the number of poles were kept the same for both generator designs. The original design has an outer diameter of 6.37 m. The diameter of the new design is smaller with 6.14 m. The new design is however wider with an axial length of 1.72 m as compared to the original design with a width of 1.34 m. The axial length had to be increased to fit the new claw poles. Overall the active mass of the generator was increased from 61 to 74 tonnes due to increasing the length of the claw poles in order

to maintain the spacing for the field winding and its cryostat. The total mass of the original design is 184 tonnes with a power output of 10 MW, the total mass for the new design is 189 tonnes with a power output of 11.7 MW. Hence, increasing the power density from 53.19 to 61.90 W kg^{-1} by adopting the new design. It was shown that the power output as well as the power density was increased while maintaining the same inner diameter as for the original design. To highlight the improvement of the new design even further it was scaled down to 10 MW. For this power rating the mass was reduced to 178 tonnes, resulting in a mass reduction of 10 tonnes.

5. Conclusions

In this paper a novel stator design to reduce the structural mass of axial flux machines was introduced. It was suggested to design the stator at an angle in order to deviate the forces in both the horizontal as well as vertical directions. By reducing the axial forces, the structural design is simplified. The design was applied to the double claw pole machine to reduce the structural mass. Further improvements could be made such as eliminating the pivoting force that existed previously on the small claw poles. Through these steps the structural mass was reduced from 126 to 115 tonnes. Additionally, to the new stator concept, new claw pole shapes were designed. The claw poles saturate later due to a bigger cross-sectional area and hence can carry more flux. A reluctance network was developed and FEA models were created in order to determine the electromagnetic performance of the machine. From the simulations the stator tooth flux was found to increase from 57 to 71.4 mWb increasing the power output of the generator from 10 to 11.7 MW. One of the major disadvantages of the double claw pole machine was its weight. Through the new design the power density of the generator was further increased from 53.19 to 61.90 W kg^{-1} making it more competitive while still maintaining the same superconducting wire requirements and its modularity.

It is believed that the double claw pole machine in conjunction with the new design and further work can lead to a cost-effective power generator for 10 MW and even higher rated wind turbines.

Acknowledgment

This work was supported by the Engineering and Physical Sciences Research Council (grant number: EPSRC EPN509644/1).

ORCID iDs

Kevin Kails https://orcid.org/0000-0002-3418-5977
Quan Li https://orcid.org/0000-0001-7153-0656

References

[1] Pineda I *et al* 2017 The European offshore wind industry—key trends and statistics 2016 *Wind Europe Annual Report* https://windeurope.org/wp-content/uploads/files/about-wind/statistics/WindEurope-Annual-Offshore-Statistics-2016.pdf
[2] IHS Emerging Energy Research 2009 Global offshore wind energy markets and strategies: 2009–2020 *Technical Report*
[3] Abrahamsen A B *et al* 2013 *INNWIND Reference Wind Turbine Report* Work Package 1—Deliverable 1.21 www.innwind.eu
[4] Keysan O and Mueller M 2015 A modular and cost-effective superconducting generator design for offshore wind turbines *Supercond. Sci. Technol.* **28** 034004
[5] Gieras J F 2008 *Advancements in Electric Machines* (Berlin: Springer)
[6] Snitchler G *et al* 2011 10 MW class superconductor wind turbine generator *IEEE Trans. Appl. Supercond.* **21** 1089–92
[7] Sung H-J *et al* 2013 Practical design of a 10 MW superconducting wind power generator considering weight issue *IEEE Trans. Appl. Supercond.* **23** 5201805
[8] Abrahamsen A B *et al* 2010 Superconducting wind turbine generators *Supercond. Sci. Technol.* **23** 034019
[9] Kostopoulos D *et al* 2013 Feasibility study of a 10 MW MgB_2 fully superconducting generator for offshore wind turbines *EWEA Offshore Conf. 2013 (Frankfurt, Germany)*
[10] Marino I *et al* 2016 Lightweight MgB_2 superconducting 10 MW wind generator *Supercond. Sci. Technol.* **29** 024005
[11] Kim J H and Kim H M 2013 Electromagnetic design of 10 MW class superconducting wind turbine using 2 G HTS wire *Prog. Supercond. Cryog.* **15** 29–34
[12] Terao Y and Sekino M 2012 Electromagnetic design of 10 MW class fully superconducting wind turbine generators *IEEE Trans. Appl. Supercond.* **22** 5201904
[13] Fair R *et al* 2012 Next generation drive train-superconductivity for large-scale wind turbines *Applied Superconductivty Conf. (Portland, OR)*
[14] Kalsi S S 2014 Superconducting wind turbine generator employing MgB_2 windings both on rotor and stator *IEEE Trans. Appl. Supercond.* **24** 5201907
[15] Abrahamsen A B *et al* 2011 Feasibility study of 5 MW superconducting wind turbine generator *Physica* C **471** 1464–9
[16] Patterson D J 2009 A comparison of radial and axial flux structures in electrical machines *Interational Electric Machines and Drives Conf. (Miami, FL)*
[17] Bang D 2010 Design of transverse flux permanent magnet machines for large direct-drive wind turbines *PhD Dissertation* Delft University of Technology
[18] Bruzzese C *et al* 2014 A finite reluctance approach to electrical machine modeling and simulation: magnetic network-based field solutions in MatLab environment *Industrial Electronics Society, IECON 2014—40th Annual Conf. of the IEEE (Dallas, TX)*
[19] Curti M, Paulides J J H and Lomonova E A 2015 An overview of analytical methods for magnetic field computation *2015 10th Int. Conf. on Ecological Vehicles and Renewable Energies (EVER) (Monte Carlo, Monaco)*
[20] Bernholz J J and Mueller M 2016 Analytical model of superconducting generators for wave energy systems *8th IET Int. Conf. on Power Electronics, Machines and Drives (Glasgow, UK)*
[21] Vacuumschmelze 2017 Vacoflux datasheet (http://vacuumschmelze.com)
[22] Zavvos A 2013 Structural optimization of permanent magnet direct drive generators for 5 MW wind turbines *PhD Thesis* University of Edinburgh
[23] Keysan O 2014 Superconducting generators for large offshore wind turbines *PhD Thesis* University of Edinburgh